

Critical Dynamics of Weakly-Dissipative Driven Systems

Daniel A. Paz* and Mohammad F. Maghrebi

Department of Physics and Astronomy, Michigan State University, East Lansing, Michigan 48824, USA

Driven quantum systems coupled to an environment typically exhibit an effectively classical behavior with relaxational dynamics at, or near, criticality. A paradigmatic driven-dissipative model is the open Dicke model which describes collective light-matter interactions and features a superradiant phase that is observed in experiments. In this work, we investigate the closely related infinite-range Ising model, in a transverse field, subject to individual atomic dissipation. This effective model governs the open Dicke model in the limit of large cavity detuning. We show that, in the weakly dissipative regime, the system undergoes a dynamical crossover from relaxational dynamics, with a characteristic dynamical exponent $\zeta = 1/2$, to underdamped critical dynamics described by the exponent $\zeta = 1/4$. We identify these critical behaviors with the infinite-range classical (stochastic) and quantum (unitary) Ising models at finite temperature, respectively. However, in contrast with the volume law ($\sim N$, the system size) expected at finite temperature, we show that the von Neumann entropy scales logarithmically with the system size at criticality, $S_{\text{vN}} = \frac{1}{4} \log N$. We nevertheless obtain a finite value for the entanglement negativity, $E_{\mathcal{N}} = \log \sqrt{2}$, thus confirming the purely classical nature of the phase transition. To obtain these results, we introduce a non-equilibrium extension of the Suzuki-Trotter quantum-to-classical mapping in the superoperator space.

The search for new physics in non-equilibrium quantum systems has been fervently ongoing in recent years. A generic setting is provided by driven quantum systems coupled to the environment—also known as driven-dissipative systems. This setting has been realized in diverse platforms such as circuit QED [1], cavity QED [2, 3], and trapped ions [4–6], among others, and has led to a flurry of theoretical efforts aiming to understand many-body open quantum systems far from equilibrium. These systems can harbor new, non-equilibrium phases of matter, and in the era of noisy intermediate-scale quantum devices [7], offer an ideal setting to study how noise affects quantum systems.

Many advances notwithstanding, it has become increasingly clear that generic driven-dissipative systems appear thermal at long-wavelengths [8–21]. This emergent classical behavior can be attributed to the repeated *measurement* (i.e. dissipation) of the quantum system by the environment leading to the loss of coherence. Conventional wisdom then says that an effectively classical behavior should emerge where the dynamics is relaxational or overdamped. On the other hand, a weakly dissipative quantum system is only measured infrequently and may exhibit coherent dynamics for a long time. This line of reasoning suggests that the dynamics in a weakly-dissipative regime *cannot* be purely relaxational.

In this work, we study the infinite-range driven-dissipative Ising model (DDIM) in a transverse field, where individual spins are subject to dissipation; similar models emerge in a limit of the paradigmatic open Dicke model where photons can be adiabatically eliminated [22–24]. Specifically, we investigate the phase transition to an ordered phase in the weakly dissipative regime. It is shown that while static properties display the same critical behavior, regardless of the strength of dissipation, the weakly dissipative phase transition ex-

hibits underdamped critical dynamics. This phase transition is governed by a distinct critical exponent, in contrast with the relaxational dynamics at a generic critical point. We identify these behaviors with the infinite-range quantum (unitary) and classical (stochastic) Ising models at finite temperature, respectively. It is nevertheless shown that entanglement negativity is finite even at the phase transition, rendering the transition strictly classical. In addition to exact numerical simulation, we employ an analytical approach based on an elegant extension of the Suzuki-Trotter quantum-to-classical mapping to the non-equilibrium realm of open quantum systems.

Model.—Consider a system of 2-level atoms with an infinite-range Ising-type interaction, in a transverse field, and coherently driven by a classical beam. In the rotating frame of the drive, the Hamiltonian H is described by the effective spin model

$$H = -\frac{J}{N} \sum_{i,j} \sigma_i^x \sigma_j^x + \Delta \sum_i \sigma_i^z, \quad (1)$$

with J the interaction strength, Δ the transverse field, and σ_i^μ the usual Pauli matrices. Given the collective nature of the interaction, the Hamiltonian can be described in terms of the total spin $S_\mu = \sum_i \sigma_i^\mu$. Furthermore, due to the coupling to the environment, atomic spontaneous emission leads to the decay of spin $|\uparrow\rangle$ to $|\downarrow\rangle$. Under the Born-Markov conditions, the dynamics is governed by the Liouvillian \mathcal{L} as [25]

$$\frac{d\rho}{dt} \equiv \mathcal{L}(\rho) = -i[H, \rho] + \sum_i (L_i \rho L_i^\dagger - \frac{1}{2} \{L_i^\dagger L_i, \rho\}), \quad (2)$$

where the (curly) brackets represent the (anti)commutator. Here, $L_i = \sqrt{\Gamma} \sigma_i^-$ is the Lindblad operator characterizing spontaneous emission at the rate Γ . This model also describes the open Dicke model in the

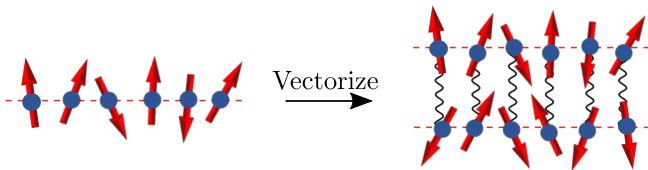


Figure 1. Schematic representation of density matrix vectorization. By purifying the quantum state, the Liouvillian dynamics of a spin chain in an open quantum system can be mimicked by a (non-Hermitian) Hamiltonian on a *ladder* of spins in a closed system. Wavy lines represent dissipation.

limit of large detuning upon adiabatic elimination of the cavity mode [22, 23, 26]; see the Supplemental Material (SM). We thus expect the results of this work to be immediately relevant to the open Dicke model. Just like the Dicke model, the DDIM has a \mathbb{Z}_2 symmetry under $\sigma^{x,y} \rightarrow -\sigma^{x,y}$. This symmetry is spontaneously broken in the transition from the normal ($\langle S_x \rangle = 0$) to the ordered phase ($\langle S_x \rangle \neq 0$).

Ultimately, we wish to characterize the collective behavior of the DDIM in the steady state at long times. To this end, we start with the non-equilibrium partition function

$$Z = \text{Tr}[\rho(t)] = \text{Tr} [e^{\mathcal{L}t}(\rho_0)],$$

where ρ_0 is the initial density matrix; notice that $Z = 1$ [27]. In order to exploit the Suzuki-Trotter decomposition, we first *vectorize* the density matrix and cast the Liouvillian \mathcal{L} as a superoperator \mathbb{L} . In this basis, the Liouvillian becomes a (non-Hermitian) Hamiltonian-like object that acts on two copies of the original system. This transformation is schematically shown for a one-dimensional spin system in Fig. 1. Vectorization maps the original spin chain to a *ladder* of spins in which the Hamiltonian only couples spins on the same (upper/lower) leg of the ladder, while dissipation couples those across rungs of the ladder [28–31]. In this mapping, the Liouvillian dynamics takes the form

$$e^{\mathcal{L}t}(\rho_0) \rightarrow e^{\mathbb{L}t} |\rho_0\rangle\rangle,$$

where the *superket* $|\rho\rangle\rangle$ denotes the vectorized density matrix. The inner product in this superoperator space is given by the Frobenius norm, $\langle\langle A|B\rangle\rangle = \text{Tr} [A^\dagger B]$, so that the non-equilibrium partition function in this basis is given by

$$Z = \text{Tr} [\rho(t)] = \langle\langle I | e^{\mathbb{L}t} |\rho_0\rangle\rangle. \quad (3)$$

Here, we have used the fact that the overlap of the density matrix with the identity in the superoperator space is equivalent to taking the trace in the original Hilbert space.

Quantum-to-Classical Mapping.—The non-equilibrium partition function in the superoperator space, Eq. (3), resembles the transition amplitude of a quantum spin system. This analogy unlocks the rich toolbox of quantum

statistical mechanics. Specifically, we adapt the Suzuki-Trotter decomposition [32] to our non-equilibrium model; this is particularly well suited to treat *individual* atomic dissipation where standard techniques fail (see [33] for an alternative approach). The first step to construct this mapping is to Trotterize the evolution operator:

$$e^{t\mathbb{L}} = \lim_{M \rightarrow \infty} (e^{\delta t \mathbb{L}_0} e^{\delta t \mathbb{L}_1})^M,$$

with $\delta t = t/M$. Here, we have split \mathbb{L} into two parts. \mathbb{L}_0 contains the diagonal terms in the σ^x basis (i.e. the Ising term), and \mathbb{L}_1 consists of the off-diagonal terms (i.e. the transverse field, as well as dissipation). Next, we follow Suzuki's procedure and insert a resolution of the identity in the diagonal basis at each time slice. This construction leads to the partition function

$$Z = \lim_{M \rightarrow \infty} \sum_{\sigma} e^{iS_0[\sigma] + iS_1[\sigma]}, \quad (4)$$

where $\sigma \equiv \{\sigma_{i,k}^{(u)}, \sigma_{i,k}^{(l)}\}$ is a shorthand for classical spin configurations. Here, $\sigma_{i,k}^{(u/l)}$ represents the i th atom at the k th time step on the upper/lower leg of the spin ladder and only assumes the discrete values ± 1 (corresponding to the eigenvalues of σ^x). The action S_0 , corresponding to the diagonal terms, takes the form

$$S_0 = \frac{J\delta t}{N} \sum_{k=0}^M \left((S_k^{(u)})^2 - (S_k^{(l)})^2 \right), \quad (5)$$

with $S_k = \sum_i \sigma_{i,k}$ the total spin. Due to the collective nature of the Ising interaction, we may utilize a Hubbard-Stratonovich transformation for each term in Eq. (5) to decouple the total spins. This will enable us to conveniently trace out the spins in order to obtain a partition function in terms of the two (Hubbard-Stratonovich) scalar fields $m_k^{(u/l)}$. In this representation the contribution from the spins is represented by a matrix $\mathbb{T}(m_k^{(u/l)})$ that encodes the time evolution of a single rung. Taking the continuum limit by sending $\delta t \rightarrow 0$ and replacing the index k with the continuous time t , the full action reads

$$\mathcal{S} = -2JN \int_t m_c(t) m_q(t) - iN \ln \text{Tr} \left[\mathcal{T} e^{\int_t \mathbb{T}(m_{c/q}(t))} \right]. \quad (6)$$

Here, \mathcal{T} denotes time ordering, and the fields $m_{c/q} = (m^{(u)} \pm m^{(l)})/\sqrt{2}$ are defined for future convenience. In the basis $|\sigma^{(u)}\rangle |\sigma^{(l)}\rangle$, the matrix \mathbb{T} is given by

$$\mathbb{T} = \begin{pmatrix} -\frac{\Gamma}{4} + i2\sqrt{2}Jm_q & i\Delta & -i\Delta & \frac{\Gamma}{4} \\ i\Delta - \frac{\Gamma}{2} & -\frac{3\Gamma}{4} + i2\sqrt{2}Jm_c & -\frac{\Gamma}{4} & -i\Delta - \frac{\Gamma}{2} \\ -i\Delta - \frac{\Gamma}{2} & -\frac{\Gamma}{4} & -\frac{3\Gamma}{4} - i2\sqrt{2}Jm_c & i\Delta - \frac{\Gamma}{2} \\ \frac{\Gamma}{4} & -i\Delta & i\Delta & -\frac{\Gamma}{4} - i2\sqrt{2}Jm_q \end{pmatrix}.$$

Contrast the 4×4 matrix against the 2×2 transfer matrix arising in the equilibrium quantum-to-classical mapping [34]; the doubling is simply due to the vectorization

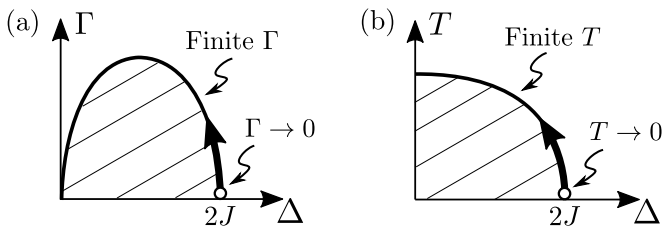


Figure 2. Phase diagrams of the infinite-range (a) driven-dissipative Ising model (DDIM), and (b) equilibrium Ising model in a transverse field. The shaded regions denote the ordered phase. The weakly dissipative critical point of the DDIM, $\Gamma \rightarrow 0$ in (a), exhibits underdamped dynamics in contrast with the relaxational dynamics at a generic critical point. Analogously, the equilibrium model in (b) exhibits distinct (quantum and thermal) dynamics at zero and finite temperature. Both $\Gamma \rightarrow 0$ and $T \rightarrow 0$ define unstable fixed points but with respect to dissipation and thermal fluctuations, respectively. The weakly dissipative dynamics in (a) exhibits identical critical scaling to a finite-temperature critical point in (b).

of the density matrix. Interestingly, our procedure has resulted in a Keldysh-like action with $m^{(u/l)}$ representing the forward/backward fields, although our starting point was quite different from the Keldysh field theoretical approach. Finally, the collective nature of the Ising interaction leads to an overall factor of N in the action, enabling us to obtain exact results from the saddle-point approximation.

Critical Properties & Finite-Size Scaling.—We first compute the magnetization through the saddle point approximation, which is exact in the limit $N \rightarrow \infty$. To this end, we set $\frac{\delta S}{\delta m_{c/q}(t)} = 0$ and seek a solution with $m_q(t) = 0$ and $m_c(t) \equiv m = \text{const}$. In the normal phase, only one stable solution exists, where $m = 0$. In the ordered phase, there are two stable solutions, $m = \pm\sqrt{-\Gamma^2 - 16\Delta^2 + 32\Delta J}/4J$, signifying the breaking of the \mathbb{Z}_2 symmetry; see the phase diagram in Fig. 2(a). (Absence of driven-dissipative phase transitions in Ising-type models at $\Delta = 0$ is generally proved in Ref. [35].) Within the normal phase, we expand the action in powers of fluctuations around $m_{c/q} = 0$. We have, up to the quadratic order,

$$\mathcal{S}^{(2)} = \frac{1}{2} \int_{t,t'} (m_c, m_q)_t \begin{pmatrix} 0 & P^A \\ P^R & P^K \end{pmatrix}_{t-t'} \begin{pmatrix} m_c \\ m_q \end{pmatrix}_{t'}, \quad (7)$$

with $(P^A(t) = P^R(-t))$

$$\begin{aligned} P^R(t) &= -2J\delta(t) + \Theta(t)8J^2e^{-\frac{\Gamma}{2}|t|} \sin(2\Delta t), \\ P^K(t) &= i8J^2e^{-\frac{\Gamma}{2}|t|} \cos(2\Delta t). \end{aligned} \quad (8)$$

In a slight abuse of notation, a factor of \sqrt{N} has been absorbed into both m_c and m_q . The above action is *exact* in the large- N limit away from the critical point—higher order terms are suppressed as $\mathcal{O}(1/N)$. We can then

investigate the auto-correlation as well as the spectral response functions:

$$\begin{aligned} C(t) &= \frac{1}{N} \langle \{S_x(t), S_x(0)\} \rangle = \langle m_c(t)m_c(0) \rangle, \\ \chi(t) &= \frac{i}{N} \langle [S_x(t), S_x(0)] \rangle = i \langle m_q(t)m_c(0) - m_c(t)m_q(0) \rangle. \end{aligned}$$

These functions can be obtained by inverting the kernel in Eq. (7). Defining the critical point $\Gamma_c = 4\sqrt{\Delta(2J - \Delta)}$ and the distance from this point $\gamma = \Gamma - \Gamma_c$, a simple analysis close to the critical point ($\gamma \ll \Gamma$) at long times ($t \gg 1/\Gamma$) yields the correlation and response functions

$$C(t) \sim \frac{16J\Delta}{\gamma\Gamma_c} e^{-\gamma|t|/2}, \quad \chi(t) \sim \text{sgn}(t) \frac{4\Delta}{\Gamma_c} e^{-\gamma|t|/2}. \quad (9)$$

The critical behavior near the phase transition can be characterized by an effective temperature via the *classical* fluctuation-dissipation relation, $\chi(t) = -\partial_t C(t)/2T_{\text{eff}}$ [36]. Equation (9) then reveals that $T_{\text{eff}} = J$ everywhere along the phase boundary. Note that correlations diverge as $1/\gamma$ upon approaching the critical point, $\gamma \rightarrow 0$, while the response function remains finite. These scaling properties determine the scaling dimensions of the fields, upon rescaling time (or inversely rescaling γ), to be $[m_c] = \frac{1}{2}$ and $[m_q] = -\frac{1}{2}$. This gives rise to a classical, relaxational dynamics near the critical point.

Next, we turn our attention to the weakly dissipative critical point where $\Gamma \rightarrow 0$ while $\Delta = 2J$. Here, the coherent dynamics is not overtaken by dissipation, and a different dynamical behavior should be expected. Indeed, we find

$$\begin{aligned} C(t) &\sim \frac{32J^2}{\Gamma^2} (2 + \Gamma|t|) e^{-\Gamma|t|/2}, \\ \chi(t) &\sim 8Jt e^{-\Gamma|t|/2}. \end{aligned} \quad (10)$$

Correlations now diverge as $1/\Gamma^2$ upon approaching the weakly dissipative critical point $\Gamma \rightarrow 0$. In addition, the response function scales linearly with t . These observations yield the scaling dimensions $[m_c] = 1$ and $[m_q] = 0$, which are distinct from those at a generic critical point discussed above and are also distinguished from the quantum critical point scaling dimensions $[m_c] = 1/2$ and $[m_q] = 1/2$ [15]. We shall see shortly that the weakly dissipative critical point is described by underdamped, rather than overdamped, dynamics.

So far, we have inspected the critical behavior near, but away from, the critical point. The divergence of the correlation function at the critical point will be regularized by the finite size of the system, but requires a finite-size scaling. To this end, we first remark that the most relevant interaction term in the action is given by the “classical vertex” $\sim \frac{1}{N} \int_t m_c^3(t)m_q(t)$ as $[m_c] > [m_q]$. Upon rescaling time ($t \rightarrow \lambda t$), this term remains invariant only if N is rescaled appropriately. Using the scaling dimensions of the fields, we find that N has to be

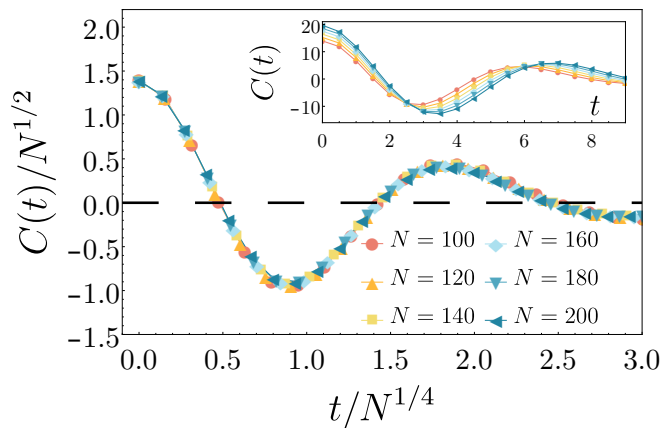


Figure 3. Finite-size scaling of the correlation function near the weakly dissipative critical point ($J = 1, \Delta = 2, \Gamma = 0.1$). The dynamics is underdamped in contrast with the purely relaxational behavior at a generic driven-dissipative phase transition, and exhibits the critical scaling $t \sim N^{1/4}$ to be contrasted with $t \sim N^{1/2}$ of relaxational dynamics.

rescaled as $N \rightarrow N' = N/\lambda^2$ at a generic critical point, while $N \rightarrow N' = N/\lambda^4$ at the weakly dissipative critical point. The correlation function at criticality can then be written as

$$C(t) = N^\alpha \mathcal{C}(t/N^\zeta), \quad (11)$$

where the exponent α dictates the scaling of fluctuations, and the exponent ζ defines a dynamical critical exponent. While *static* fluctuations always scale as $N^{1/2}$, identifying $\alpha = 1/2$, the generic and weakly dissipative critical points are characterized by two distinct *dynamical* exponents, $\zeta = 1/2$ and $\zeta = 1/4$, respectively. Furthermore, the latter exhibits underdamped critical dynamics (Fig. 3), while a generic critical point is purely relaxational; see the SM. This indicates that the quantum coherent dynamics persists at weak dissipation, although static correlations exhibit an effective thermal behavior [15]. Interestingly, the critical behavior in the weakly dissipative regime can be identified with the infinite-range *quantum* Ising model in a transverse field but at finite temperature, see the SM. In contrast, the critical behavior at a generic critical point can be identified with the infinite-range *classical* Ising model with (stochastic) Glauber dynamics [37]. For a comparison, see Table I. While an effective classical behavior is expected even in a quantum system at a thermal critical point [38], the above models are special due to the infinite-range interactions; see also our discussion of integrability.

The limit $\Gamma \rightarrow 0$ in the weakly dissipative regime may appear unphysical; however, the underdamped critical scaling emerges even at a finite strength of dissipation as long as $\Gamma t \lesssim 1$ and $\Gamma \lesssim N^{-1/4}$. A dynamical crossover to overdamped relaxational dynamics is then expected at longer times and larger systems. In Fig. 3, we have

	Driven-Diss.		Class.	Quantum	
	$\Gamma > 0$	$\Gamma \rightarrow 0$	$T > 0$	$T > 0$	$T \rightarrow 0$
$t \sim N^\zeta$	$\frac{1}{2}$	$\frac{1}{4}$	$\frac{1}{2}$	$\frac{1}{4}$	$\frac{1}{3}$
$C \sim N^\alpha$	$\frac{1}{2}$	$\frac{1}{2}$	$\frac{1}{2}$	$\frac{1}{2}$	$\frac{1}{3}$
vN Entropy	$\frac{1}{4} \log N$		vol.	vol.	$\frac{1}{6} \log N$
Log. Negativity	$\log \sqrt{2}$		0	const.	$\frac{1}{6} \log N$

Table I. Driven-dissipative vs. equilibrium classical/ quantum Ising models. A generic (finite- Γ) critical point exhibits the same critical behavior as the classical stochastic Ising model, while the weakly dissipative ($\Gamma \rightarrow 0$) critical point can be identified with the quantum Ising model at finite temperature. In both regimes of the driven-dissipative model, the von Neumann entropy scales as $\frac{1}{4} \log N$ in contrast with the volume law at finite temperature, while the negativity assumes a finite value, affirming the classical nature of the phase transition.

identified the underdamped dynamics and a universal dynamical scaling at a finite, yet small value of $\Gamma/J = 0.1$ where $Jt \lesssim 10$ and $N \lesssim 200$. A qualitative analogy can be made with the quantum-to-classical crossover at finite temperature [39]. Indeed, both quantum and weakly dissipative critical points define unstable fixed points with respect to thermal fluctuations and dissipation, in and out of equilibrium, respectively; see Fig. 2.

Entanglement.—Driven-dissipative systems tend to behave classically near the phase transition. The weakly dissipative point is rather special in that the system is infrequently measured by the environment. Furthermore, the critical point of our driven-dissipative model in the limit $\Gamma \rightarrow 0$ coincides exactly with the quantum critical point of the transverse-field Ising model (both at $\Delta = 2J$); see Fig. 2. This curious fact naturally leads one to suspect whether the quantum character of the model survives in the weakly dissipative regime. To characterize quantum correlations, we investigate the entanglement.

We first report the characteristic behavior of the von Neumann entropy of a subsystem near criticality. This quantity is a true measure of entanglement only in a pure state (such as the ground state), but it still provides characteristic information about (quantum and classical) correlations in a mixed state, in this case the steady state of our driven-dissipative model. We find that $S_{\text{vN}} \sim \frac{1}{4} \log N$ everywhere along the phase boundary, which is to be contrasted with both the quantum [40] and classical cases; see Table I and the detailed derivation in the SM. The mutual information, however, is the same ($\sim \frac{1}{4} \log N$) as that of the Ising model at finite temperature [41].

To identify the quantum nature of the phase transition, we consider logarithmic negativity as a measure of quantum entanglement suited to mixed states [42]. Surprisingly, we find that this quantity assumes the same value $E_{\mathcal{N}} = \log \sqrt{2}$ everywhere along the phase bound-

ary. This parallels the behavior of the effective temperature ($T_{\text{eff}} = J = \text{const}$), which hints at a deeper connection. Nevertheless, the finite value of negativity at the critical point underscores the classical nature of the phase transition [44]. This result complements the finite atom-photon entanglement in the full Dicke model [45].

Integrability.—It has been argued recently that generic driven-dissipative systems with weak dissipation approach a thermal (Gibbs) state [46]. In contrast, the infinite-range Ising Hamiltonian considered in this work is integrable [47]. While we have identified an *effective* thermal behavior, the steady state cannot be described as a thermal state, $e^{-H/T}$ with H the Ising Hamiltonian (1). This is particularly evident at $\Delta = 2J$. While this point defines a quantum critical point in equilibrium at $T = 0$, we have identified, using the fluctuation-dissipation relation, a finite effective temperature $T_{\text{eff}} = J$.

Summary and Outlook.—In this work, we have considered a driven-dissipative Ising model with infinite-range interactions, relevant to existing experimental platforms. We have shown that the critical dynamics becomes underdamped in the weakly dissipative regime, in contrast with the relaxational dynamics at a generic critical point. We have further shown that the two are governed by distinct dynamical exponents, which are identified with those of the infinite-ranged quantum and classical Ising models at finite temperature. By inspecting entanglement, we have shown that the phase transition is of a classical nature even in the weakly dissipative regime. Extension of this work to the full open Dicke model outside the domain of adiabatic elimination is a natural direction for future research. The interplay of weakly dissipative dynamics and integrability constitutes another interesting topic for investigation [48]. Finally, the emergence of quantum critical behavior in driven-dissipative systems defines an important future direction [49].

Acknowledgements.—This material is based upon work supported by the NSF under Grant No. DMR-1912799. The authors also acknowledge the start-up funding from Michigan State University. We are also indebted to Alireza Seif and Paraj Titum for valuable discussions.

* Corresponding author: pazdanie@msu.edu

[1] M. Fitzpatrick, N. M. Sundaresan, A. C. Li, J. Koch, and A. A. Houck, *Phys. Rev. X* **7**, 011016 (2017).
 [2] K. Baumann, C. Guerlin, F. Brennecke, and T. Esslinger, *Nature* **464**, 1301 (2010).
 [3] M. P. Baden, K. J. Arnold, A. L. Grimsmo, S. Parkins, and M. D. Barrett, *Phys. Rev. Lett.* **113**, 020408 (2014).
 [4] J. T. Barreiro, M. Miller, P. Schindler, D. Nigg, T. Monz, M. Chwalla, M. Hennrich, C. F. Roos, P. Zoller, and R. Blatt, *Nature* **470**, 486 (2011).
 [5] Y. Lin, J. P. Gaebler, F. Reiter, T. R. Tan, R. Bowler, A. S. Srensen, D. Leibfried, and D. J. Wineland, *Nature* **504**, 415 (2013).

[6] A. Safavi-Naini, R. J. Lewis-Swan, J. G. Bohnet, M. Gärttner, K. A. Gilmore, J. E. Jordan, J. Cohn, J. K. Freericks, A. M. Rey, and J. J. Bollinger, *Phys. Rev. Lett.* **121**, 040503 (2018).
 [7] J. Preskill, *Quantum* **2**, 79 (2018).
 [8] A. Mitra, S. Takei, Y. B. Kim, and A. J. Millis, *Phys. Rev. Lett.* **97**, 236808 (2006).
 [9] M. Wouters and I. Carusotto, *Phys. Rev. B* **74**, 245316 (2006).
 [10] S. Diehl, A. Micheli, A. Kantian, B. Kraus, H. Büchler, and P. Zoller, *Nature Physics* **4**, 878 (2008).
 [11] S. Gopalakrishnan, B. L. Lev, and P. M. Goldbart, *Phys. Rev. A* **82**, 043612 (2010).
 [12] D. Nagy, G. Szirmai, and P. Domokos, *Phys. Rev. A* **84**, 043637 (2011).
 [13] B. Oztop, M. Bordyuh, O. E. Mustecaplioglu, and H. E. Tureci, *New J. Phys.* **14**, 085011 (2012).
 [14] E. G. Dalla Torre, E. Demler, T. Giamarchi, and E. Altman, *Phys. Rev. B* **85**, 184302 (2012).
 [15] E. G. Dalla Torre, S. Diehl, M. D. Lukin, S. Sachdev, and P. Strack, *Phys. Rev. A* **87**, 023831 (2013).
 [16] L. M. Sieberer, S. D. Huber, E. Altman, and S. Diehl, *Phys. Rev. Lett.* **110**, 195301 (2013).
 [17] M. F. Maghrebi and A. V. Gorshkov, *Phys. Rev. B* **93**, 014307 (2016).
 [18] M. Foss-Feig, P. Niroula, J. T. Young, M. Hafezi, A. V. Gorshkov, R. M. Wilson, and M. F. Maghrebi, *Phys. Rev. A* **95**, 043826 (2017).
 [19] L. M. Sieberer, M. Buchhold, and S. Diehl, *Rep. Prog. Phys.* **79**, 096001 (2016).
 [20] D. Kilda and J. Keeling, *Phys. Rev. Lett.* **122**, 043602 (2019).
 [21] P. Kirton, M. M. Roses, J. Keeling, and E. G. Dalla Torre, *Adv. Quantum Technol.* **2**, 1800043 (2019).
 [22] J. Keeling, M. J. Bhaseen, and B. D. Simons, *Phys. Rev. Lett.* **105**, 043001 (2010).
 [23] F. Damanet, A. J. Daley, and J. Keeling, *Phys. Rev. A* **99**, 033845 (2019).
 [24] D. Barberena, R. J. Lewis-Swan, J. K. Thompson, and A. M. Rey, *Phys. Rev. A* **99**, 053411 (2019).
 [25] H.-P. Breuer and F. Petruccione, *The Theory of Open Quantum Systems* (Oxford University Press, 2002).
 [26] S. Morrison and A. S. Parkins, *Phys. Rev. Lett.* **100**, 040403 (2008).
 [27] A. Kamenev, *Field theory of non-equilibrium systems* (Cambridge University Press, 2011).
 [28] V. Tarasov, *Quantum mechanics of non-hamiltonian and dissipative systems*, Vol. 7 (Elsevier, 2008).
 [29] T. c. v. Prosen and I. Pižorn, *Phys. Rev. Lett.* **101**, 105701 (2008).
 [30] M. Žnidarič, *Phys. Rev. E* **89**, 042140 (2014).
 [31] M. Žnidarič, *Phys. Rev. E* **92**, 042143 (2015).
 [32] M. Suzuki, *Prog. Theor. Phys.* **56**, 1454 (1976).
 [33] E. G. Dalla Torre, Y. Shchadilova, E. Y. Wilner, M. D. Lukin, and E. Demler, *Phys. Rev. A* **94**, 061802 (2016).
 [34] S. Suzuki, J.-i. Inoue, and B. K. Chakrabarti, *Quantum Ising Phases and Transitions in Transverse Ising Models*, 2nd ed., Lecture Notes in Physics (Springer-Verlag, Berlin Heidelberg, 2013).
 [35] M. Foss-Feig, J. T. Young, V. V. Albert, A. V. Gorshkov, and M. F. Maghrebi, *Phys. Rev. Lett.* **119**, 190402 (2017).
 [36] U. C. Täuber, *Critical Dynamics: A Field Theory Approach to Equilibrium and Non-Equilibrium Scaling Be-*

- havior* (Cambridge University Press, 2014).
- [37] S. K. Oh and Kang, Hee Jae, *J. Korean Phys. Soc.* **47**, 6 (2005).
 - [38] B. I. Halperin and P. C. Hohenberg, *Phys. Rev.* **177**, 952 (1969).
 - [39] S. Sachdev, *Quantum Phase Transitions* (Cambridge University Press, 2011).
 - [40] T. Barthel, S. Dusuel, and J. Vidal, *Phys. Rev. Lett.* **97**, 220402 (2006).
 - [41] J. Wilms, J. Vidal, F. Verstraete, and S. Dusuel, *J. Stat. Mech.: Theory Exp* **2012**, P01023 (2012).
 - [42] G. Vidal and R. F. Werner, *Phys. Rev. A* **65**, 032314 (2002).
 - [43] H. Wichterich, J. Vidal, and S. Bose, *Phys. Rev. A* **81**, 032311 (2010).
 - [44] N. E. Sherman, T. Devakul, M. B. Hastings, and R. R. P. Singh, *Phys. Rev. E* **93**, 022128 (2016).
 - [45] E. Wolfe and S. F. Yelin, *Phys. Rev. Lett.* **112**, 140402 (2014).
 - [46] T. Shirai and T. Mori, [arXiv:1812.09713](https://arxiv.org/abs/1812.09713) (2018).
 - [47] P. Leboeuf and A. Voros, *J. Phys. A* **23**, 1765 (1990).
 - [48] F. Lange, Z. Lenarčič, and A. Rosch, *Nat. Commun.* **8**, 15767 (2017).
 - [49] J. Marino and S. Diehl, *Phys. Rev. Lett.* **116**, 070407 (2016).

Supplemental Material

In this supplemental material, we provide a detailed derivation of the quantum-to-classical mapping and the Keldysh action (Sec. I), saddle-point equations (Sec. II), effective temperature (Sec. III), and correlation functions (Sec. IV). We then derive the covariance matrix and compute the von Neumann entropy and negativity (Sec. V), introduce our numerical scheme that takes advantage of the permutation symmetry for large system-size simulations, and numerically find the scaling behavior of the dynamics in the infinite-range Ising model in a transverse field at a thermal phase transition (Sec. VI). Finally, we show explicitly how to retrieve the driven-dissipative Ising model from the open Dicke model (Sec. VII).

I. KELDYSH ACTION FROM QUANTUM-TO-CLASSICAL MAPPING

We reintroduce the driven-dissipative infinite-range Ising model whose coherent dynamics is given in terms of the Hamiltonian (in the rotating frame of the drive)

$$H = -\frac{J}{N} S_x^2 + \Delta S_z. \quad (\text{S1})$$

Here, $S_\mu = \sum_i \sigma_i^\mu$ where σ^μ , for $\mu \in \{x, y, z\}$, are the typical Pauli matrices. The full dynamics is governed by the Liouvillian

$$\mathcal{L}[\bullet] = -i[H, \bullet] + \Gamma \sum_i \left(\sigma_i^- \bullet \sigma_i^+ - \frac{1}{2} \{ \sigma_i^+ \sigma_i^-, \bullet \} \right). \quad (\text{S2})$$

It is clear that this Liouvillian does not conserve the total spin due to the presence of atomic spontaneous emission, so we cannot make use of the Holstein-Primakoff transformation. Instead, we begin by writing the Liouvillian in the superoperator space according to the rule $A|i\rangle\langle j|B \rightarrow A|i\rangle \otimes B^T|j\rangle$, where $|i\rangle\langle j|$ in the density matrix ρ is mapped to the *superket* $|i\rangle \otimes |j\rangle \equiv |i\rangle|j\rangle \equiv |i, j\rangle$ in the vectorized density matrix $|\rho\rangle\rangle$. Under this transformation, the Liouvillian acts as a matrix on the vectorized density matrix. In this *superoperator* basis, the Liouvillian takes the form

$$\mathbb{L} = -i(H \otimes I - I \otimes H) + \Gamma \sum_i \left[\sigma_i^- \otimes \sigma_i^- - \frac{1}{2} (\sigma_i^+ \sigma_i^- \otimes I + I \otimes \sigma_i^+ \sigma_i^-) \right], \quad (\text{S3})$$

where I is the identity matrix. This operator can be interpreted as a non-Hermitian Hamiltonian that acts on two copies of the system; see Fig. 1 in the main text. In our model, the Liouvillian superoperator describes infinite-range interactions along the upper/lower leg, while the two spins on each rung are coupled via dissipation. In this basis, the partition function at a given time t is

$$Z[\rho(t)] = \text{Tr}[\rho(t)] = \text{Tr} [e^{t\mathcal{L}}(\rho_0)] = \langle\langle I | e^{t\mathbb{L}} | \rho_0 \rangle\rangle. \quad (\text{S4})$$

To obtain the last equality, we have used the fact that in this vectorized space the inner product between vectors is equivalent to the Frobenius norm in the original space, $\text{Tr}[A^\dagger B] = \langle\langle A|B\rangle\rangle$. Next, we Trotterize the evolution operator $e^{t\mathbb{L}}$ and split the exponential into two parts, one including the Ising term and the other containing everything else,

$$e^{t\mathbb{L}} = \lim_{M \rightarrow \infty} (e^{\delta t \mathbb{L}_0} e^{\delta t \mathbb{L}_1})^M, \quad (\text{S5})$$

with $\delta t = t/M$. At this point, we insert resolutions of the identity at each time slice, choosing the basis that diagonalizes the Ising term. For a single time step, the corresponding matrix element is given by

$$\langle\{ \sigma_k^{(u)} \} | \{ \sigma_k^{(l)} \} | e^{\delta t \mathbb{L}_0} e^{\delta t \mathbb{L}_1} | \{ \sigma_{k-1}^{(u)} \} \rangle \rangle | \{ \sigma_{k-1}^{(l)} \} \rangle \rangle, \quad (\text{S6})$$

with the collection $\{ \sigma_k^{(u/l)} \}$ representing the set of discrete spin values (or eigenvalues of σ^x) $\sigma_{i,k}^{(u/l)} \in \{-1, 1\}$ at site i , time step k , and on the upper/lower leg of the spin ladder, respectively. The operator \mathbb{L}_0 , being diagonal, acts trivially in this basis, leading to a classical action $\exp(i\mathcal{S}_0)$ in terms of discrete spins,

$$\mathcal{S}_0 = \frac{\delta t J}{N} \sum_k \left((S_k^{(u)})^2 - (S_k^{(l)})^2 \right), \quad (\text{S7})$$

where $S_k^{(u/l)} = \sum_i \sigma_{i,k}^{(u/l)}$. In an exact fashion, we can perform the Hubbard-Stratonovich transformation (up to a normalization constant) to introduce a real scalar field $m_k^{(u/l)}$,

$$e^{iS_k} \rightarrow \int_{-\infty}^{\infty} dm_k^{(u)} dm_k^{(l)} \exp \left[-iJ\delta t N \left((m_k^{(u)})^2 - (m_k^{(l)})^2 \right) + i2J\delta t \left(m_k^{(u)} S_k^{(u)} - m_k^{(l)} S_k^{(l)} \right) \right], \quad (\text{S8})$$

which has the benefit of decoupling the Ising term. We can now trace out the discrete spins at the single-site level and represent our partition function in terms of the fields $m_k^{(u/l)}$ along with a single-site matrix $\mathbb{T}(m_k^{(u/l)}) \equiv \mathbb{T}_k$,

$$Z[\rho(t)] \sim \lim_{M \rightarrow \infty} \int_{-\infty}^{\infty} \prod_{k=0}^M dm_k^{(u)} dm_k^{(l)} e^{-i2J\delta t N \left((m_k^{(u)})^2 - (m_k^{(l)})^2 \right)} \times \left(\langle \langle I | \prod_{k'=0}^M e^{\mathbb{T}_{k'}} | \rho_0 \rangle \rangle \right)^N, \quad (\text{S9})$$

where the contribution of all sites gives rise to the power N . To obtain the single-site matrix, we take advantage of the $M \rightarrow \infty$ limit and $\delta t \rightarrow 0$ to combine all single-site exponential operators. \mathbb{T}_k then takes the form

$$\mathbb{T}_k = i2J \left(m_k^{(u)} \sigma^{x(u)} - m_k^{(l)} \sigma^{x(l)} \right) - i\Delta \left(\sigma^{z(u)} - \sigma^{z(l)} \right) + \Gamma \sigma^{-(u)} \sigma^{-(l)} - \frac{\Gamma}{2} \left(\sigma^{+(u)} \sigma^{-(u)} + \sigma^{+(l)} \sigma^{-(l)} \right), \quad (\text{S10})$$

where we have used the compact notation $O^{(u)} = O \otimes I$, $O^{(l)} = I \otimes O$. Finally, we take the continuum limit ($\delta t \rightarrow 0$). Without loss of generality, we also assume that the initial state ρ_0 is given at $t = -\infty$. These limits provide us with the final form of the partition function

$$Z = \int \mathcal{D}[m_c(t), m_q(t)] e^{i\mathcal{S}[m_c/q(t)]}, \quad (\text{S11})$$

with the Keldysh action

$$\mathcal{S} = -2JN \int_t m_c(t) m_q(t) - iN \ln \text{Tr} \left[\mathcal{T} e^{\int_t \mathbb{T}(m_c/q(t))} \right]. \quad (\text{S12})$$

Here we have introduced the *Keldysh rotation* $m_{c/q} = (m^u \pm m^l)/\sqrt{2}$ for future convenience, and absorbed all prefactors into the measure $\mathcal{D}[m_c(t), m_q(t)]$. The trace in the last term is due to a simplification as we are only interested in the steady state at late times with no memory of the initial state. The time-ordering operator \mathcal{T} also makes its appearance in the continuum limit due to the dependence of the fields on time. Finally, the explicit form of the matrix $\mathbb{T}(m^u/l(t)) \equiv \mathbb{T}(t)$ in the $|\sigma^{(u)}\rangle |\sigma^{(l)}\rangle$ basis is given by

$$\mathbb{T}(t) = \begin{pmatrix} -\frac{\Gamma}{4} + i2\sqrt{2}Jm_q(t) & i\Delta & -i\Delta & \frac{\Gamma}{4} \\ i\Delta - \frac{\Gamma}{2} & -\frac{3\Gamma}{4} + i2\sqrt{2}Jm_c(t) & -\frac{\Gamma}{4} & -i\Delta - \frac{\Gamma}{2} \\ -i\Delta - \frac{\Gamma}{2} & -\frac{\Gamma}{4} & -\frac{3\Gamma}{4} - i2\sqrt{2}Jm_c(t) & i\Delta - \frac{\Gamma}{2} \\ \frac{\Gamma}{4} & -i\Delta & i\Delta & -\frac{\Gamma}{4} - i2\sqrt{2}Jm_q(t) \end{pmatrix}. \quad (\text{S13})$$

II. SADDLE-POINT APPROXIMATION

Due to the overall factor of N in Eq. (S12), the saddle-point approximation $\delta\mathcal{S}/\delta m_{c/q}(t) = 0$ becomes exact in the thermodynamic limit and yields a solution of the form $m_q(t) = 0$ and $m_c(t) = m = \text{const}$. The constant m constitutes the order parameter of the system, and can be obtained as

$$\begin{aligned} \frac{\delta\mathcal{S}}{\delta m_q(t)} \Big|_{\substack{m_c=m \\ m_q=0}} &= -2JNm - iN \frac{\text{Tr} \left(e^{(t_f-t)\mathbb{T}_0} \mathbb{T}_q e^{(t-t_i)\mathbb{T}_0} \right)}{\text{Tr} \left(e^{(t_f-t_i)\mathbb{T}_0} \right)} \\ &= -2JNm - iN \langle \langle I | \mathbb{T}_q | \rho_{\text{ss}} \rangle \rangle = 0, \end{aligned} \quad (\text{S14})$$

where $t_{i,f}$ denote the initial and final times, respectively, which can be conveniently taken to be $\mp\infty$. Here, and in the subsequent analysis, we use the notation

$$\mathbb{T}_0 = \mathbb{T} \Big|_{m_c(t)=m, m_q(t)=0}, \quad (\text{S15})$$

$$\mathbb{T}_c = \frac{\partial \mathbb{T}}{\partial m_c(t)} \Big|_{m_c(t)=m, m_q(t)=0} = i2\sqrt{2}J \text{diag}\{0, 1, -1, 0\}, \quad (\text{S16})$$

$$\mathbb{T}_q = \frac{\partial \mathbb{T}}{\partial m_q(t)} \Big|_{m_c(t)=m, m_q(t)=0} = i2\sqrt{2}J \text{diag}\{1, 0, 0, -1\}, \quad (\text{S17})$$

with all the matrices evaluated at the saddle-point field values. To obtain the second line of Eq. (S14), we have used the long-time limit along with the fact that the only non-negative eigenvalue of \mathbb{T}_0 is zero (corresponding to the steady state), leaving us with an inner product of the corresponding left and right eigenvectors $\langle\langle I |$ (representing the identity) and $|\rho_{ss}\rangle\rangle$ (denoting the steady state). The identity vector is simply $\langle\langle I | = (1, 0, 0, 1)$, and the steady-state vector is given by

$$|\rho_{ss}\rangle\rangle = \left(\frac{8\sqrt{2}\Delta Jm}{\Gamma^2 + 16\Delta^2 + 16J^2m^2} + \frac{1}{2}, -\frac{\Gamma^2 + 16\Delta^2 + 4i\sqrt{2}\Gamma Jm}{2\Gamma^2 + 32\Delta^2 + 32J^2m^2}, \right. \\ \left. -\frac{\Gamma^2 + 16\Delta^2 - 4i\sqrt{2}\Gamma Jm}{2(\Gamma^2 + 16\Delta^2 + 16J^2m^2)}, \frac{1}{2} - \frac{8\sqrt{2}\Delta Jm}{\Gamma^2 + 16\Delta^2 + 16J^2m^2} \right)^T. \quad (\text{S18})$$

These two vectors are normalized such that $\langle\langle I | \rho_{ss}\rangle\rangle = 1$. Using Eq. (S14), we have $m = 0$ in the normal phase, while $m = \pm\sqrt{-\Gamma^2 - 16\Delta^2 + 32\Delta J}/4J$ in the ordered phase.

III. QUADRATIC EXPANSION & EFFECTIVE TEMPERATURE

We can now expand Eq. (S12) to quadratic order in fluctuations about $m = 0$ in the normal phase; below, \mathbb{T}_0 should be understood to be evaluated with $m = 0$. The expansion reads

$$\mathcal{S}^{(2)} = \frac{1}{2} \int_{t,t'} (m_c, m_q)_t \begin{pmatrix} 0 & P^A \\ P^R & P^K \end{pmatrix}_{t-t'} \begin{pmatrix} m_c \\ m_q \end{pmatrix}_{t'}, \quad (\text{S19})$$

where a factor of \sqrt{N} is absorbed into each field for convenience. The inverse Keldysh retarded/advanced response and correlation functions are (as stated in Eq. (8) in the main text)

$$P^R(t) = P^A(-t) = \frac{\delta \mathcal{S}}{\delta m_q(t) \delta m_c(0)} \Big|_{\substack{m_c=0 \\ m_q=0}} = -2J\delta(t) - i\Theta(t) \langle\langle I | \mathbb{T}_q e^{t\mathbb{T}_0} \mathbb{T}_c | \rho_{ss}\rangle\rangle \\ = -2J\delta(t) + \Theta(t) 8J^2 e^{-\frac{\Gamma}{2}t} \sin(2\Delta t), \quad (\text{S20})$$

$$P^K(t) = \frac{\delta \mathcal{S}}{\delta m_q(t) \delta m_q(0)} \Big|_{\substack{m_c=0 \\ m_q=0}} = -i \langle\langle I | \mathbb{T}_q e^{|t|\mathbb{T}_0} \mathbb{T}_q | \rho_{ss}\rangle\rangle \\ = i8J^2 e^{-\frac{\Gamma}{2}|t|} \cos(2\Delta t). \quad (\text{S21})$$

We have used the fact that, in the normal phase, the steady-state vector takes a simple form, $|\rho_{ss}\rangle\rangle = (1, -1, -1, 1)^T/2$. The step function, $\Theta(t)$, enforces the proper ordering of the matrices in Eq. (S20), stemming from $\langle\langle I | \mathbb{T}_c \exp(t\mathbb{T}_0) \mathbb{T}_q | \rho_{ss}\rangle\rangle = 0$ for all times t . Having absorbed a factor of \sqrt{N} into the fields, higher order terms are suppressed as $\mathcal{O}(1/N)$ meaning that Eq. (S19) is exact in the thermodynamic limit.

Near the critical point, the system can be assigned an effective temperature T_{eff} by imposing the fluctuation-dissipation relation [1–3]

$$P^K(\omega) = F(\omega)(P^R(\omega) - P^A(\omega)). \quad (\text{S22})$$

The inverse correlation and response functions in Fourier space are given by [we have defined the Fourier transform of the fields as $m_{c/q}(t) = \int \frac{d\omega}{2\pi} m_{c/q}(\omega) e^{-i\omega t}$]

$$P^R(\omega) = P^A(\omega)^* = -2J - 4iJ^2 \left(\frac{1}{-\Gamma/2 - i(2\Delta - \omega)} - \frac{1}{-\Gamma/2 + i(2\Delta + \omega)} \right), \quad (\text{S23})$$

$$P^K(\omega) = 4iJ^2 \Gamma \left(\frac{1}{\Gamma^2/4 + (\omega - 2\Delta)^2} + \frac{1}{\Gamma^2/4 + (\omega + 2\Delta)^2} \right). \quad (\text{S24})$$

One can see that the distribution function $F(\omega) = P^K(\omega)/(P^R(\omega) - P^A(\omega))$ at low frequencies can be described as $F(\omega) \sim 2T_{\text{eff}}/\omega$, allowing us to introduce the effective temperature

$$T_{\text{eff}} = \frac{\Gamma^2 + 16\Delta^2}{32\Delta}. \quad (\text{S25})$$

Using the (mean-field) equation for the onset of ordering, $\Gamma^2 + 16\Delta^2 - 32\Delta J = 0$, we find that $T_{\text{eff}} = J$ everywhere along the phase boundary.

IV. CRITICAL BEHAVIOR

To identify the scaling behavior, we require the correlation function

$$C(\omega) = \frac{1}{N} \mathcal{F}_\omega \langle \{S_x(t), S_x(0)\} \rangle = \frac{-iP^K(\omega)}{P^R(\omega)P^A(\omega)}, \quad (\text{S26})$$

where \mathcal{F} denotes the Fourier transform. Plugging in the inverse correlation and response functions defined in Eqs. (S23) and (S24), we obtain

$$C(\omega) = \frac{\Gamma(\Gamma^2 + 4(4\Delta^2 + \omega^2))}{2(\omega - \omega_1)(\omega - \omega_2)(\omega - \omega_3)(\omega - \omega_4)}. \quad (\text{S27})$$

The denominator here corresponds to the four poles of the correlation function, two due to the retarded and two due to the advanced response function. These poles are given by

$$\begin{aligned} \omega_1 &= -\frac{i}{2}(\Gamma - \Gamma_c), & \omega_2 &= \frac{i}{2}(\Gamma - \Gamma_c), \\ \omega_3 &= -\frac{i}{2}(\Gamma + \Gamma_c), & \omega_4 &= \frac{i}{2}(\Gamma + \Gamma_c), \end{aligned} \quad (\text{S28})$$

where $\Gamma_c = 4\sqrt{(2J - \Delta)\Delta}$. Performing the contour integral, we obtain the correlation function in the time domain:

$$C(t) = \frac{e^{-\Gamma|t|/2}}{\Gamma_c} \left(\frac{\Gamma\Gamma_c + 16(J - \Delta)\Delta}{\Gamma + \Gamma_c} e^{-\Gamma_c|t|/2} + \frac{\Gamma\Gamma_c - 16(J - \Delta)\Delta}{\Gamma - \Gamma_c} e^{\Gamma_c|t|/2} \right). \quad (\text{S29})$$

Near the critical point ($\gamma \equiv \Gamma - \Gamma_c \ll \Gamma \sim J, \Delta$), the correlation function scales as

$$C(t) \sim \frac{16J\Delta}{\gamma\Gamma_c} e^{-\gamma|t|/2}. \quad (\text{S30})$$

On the other hand, at the weakly-dissipative critical point ($\Gamma_c \rightarrow 0$ and $\Gamma \ll J, \Delta$), we find a different scaling behavior

$$C(t) \sim \frac{32J^2}{\Gamma^2} (2 + \Gamma|t|) e^{-\Gamma|t|/2}. \quad (\text{S31})$$

Note the difference in the scaling dimension under rescaling of time ($t \rightarrow \lambda t$). Similarly, we can compute the scaling dimension of the response function

$$\chi(\omega) = \frac{i}{N} \mathcal{F}_\omega \langle [S^x(t), S^x(0)] \rangle = \frac{1}{P^A(\omega)} - \frac{1}{P^R(\omega)}. \quad (\text{S32})$$

Inserting the inverse retarded and advanced response functions, we obtain

$$\chi(\omega) = 4\Delta \left(\frac{1}{(\omega - \omega_2)(\omega - \omega_4)} - \frac{1}{(\omega - \omega_1)(\omega - \omega_3)} \right). \quad (\text{S33})$$

Fourier transforming back to the time domain, the response function takes the form

$$\chi(t) = \text{sgn}(t) \frac{4\Delta}{\Gamma_c} e^{-\Gamma|t|/2} \left(e^{\Gamma_c|t|/2} - e^{-\Gamma_c|t|/2} \right). \quad (\text{S34})$$

Near the critical point, and at long times, the system behaves in an effectively thermal fashion (see Sec. III, and specifically Eq. (S25)), and we must recover the (high-temperature) fluctuation-dissipation relation $\chi(\omega) = i\omega C(\omega)/2T$, or in the time domain $\chi(t) = -\partial_t C(t)/2T$ [4]. Keeping the slowest term in both correlation and response functions, we indeed find that this equation is satisfied by identifying the effective temperature $T_{\text{eff}} = J$ at both generic and weakly dissipative critical points; see Fig. S2.

V. ENTANGLEMENT

In this section, we first calculate entanglement characteristics at the quadratic level away from the critical point. We then take advantage of the finite-size scaling relations discussed in the main text to identify the scaling behavior at criticality. We must mention that our numerical techniques based on the superoperator space are not suited for such calculations, instead we provide analytical results.

A. Covariance Matrix

Calculating the entanglement of a Gaussian state requires knowledge of the covariance matrix in a bipartitioned system [5–7]

$$C_{i,j} = \langle X_i X_j \rangle, \quad (\text{S35})$$

where $X_i \in \{q_c^A, q_c^B, p_c^A, p_c^B\}$ with q and p representing two canonically conjugate variables. The superscripts A and B denote two subsystems of equal size $N/2$. In the normal phase, the large spin is almost fully polarized along the z direction, $S_z \approx -N$, and thus the spin commutation relation reads $[S_x, S_y] \approx -2iN$. We can thus identify the canonical variables as $q \equiv S_x/\sqrt{2N}$ and $p \equiv -S_y/\sqrt{2N}$.

In order to obtain the correlation functions of the bipartitioned system, we couple source fields [2, 3], $\alpha^{A/B}(t)$ and $\beta^{A/B}(t)$, to $S_x^{A/B}$ and $-S_y^{A/B}$, respectively. Derivatives of the generating functional $W = -i \ln Z$ with respect to the sources give the connected correlation functions. The source fields must be different along the upper/lower leg of the ladder (i.e. $\alpha^{(u)} \neq \alpha^{(l)}$) so that the partition function is not equal to unity. We can then follow the same steps detailed in Sec. I to find the quantum-to-classical mapping, including the sources, in an even bipartition of the system; this yields the action

$$\mathcal{S} = -2N \int_t m_c(t) m_q(t) - i \frac{N}{2} \log \text{Tr} \left(\mathcal{T} e^{\int_t \mathbb{T}'_A(t)} \right) - i \frac{N}{2} \log \text{Tr} \left(\mathcal{T} e^{\int_t \mathbb{T}'_B(t)} \right). \quad (\text{S36})$$

In obtaining this equation, the Hubbard-Stratonovich transformation is performed on the entire system rather than each partition separately. The transfer matrices with the source fields are

$$\mathbb{T}'(t) = \mathbb{T}(m_{c/q}(t)) + \frac{1}{\sqrt{2}} \begin{pmatrix} i2\alpha_q & \beta_c - \beta_q & \beta_c + \beta_q & 0 \\ -\beta_c + \beta_q & i2\alpha_c & 0 & \beta_c + \beta_q \\ -\beta_c - \beta_q & 0 & -i2\alpha_c & \beta_c - \beta_q \\ 0 & -\beta_c - \beta_q & -\beta_c + \beta_q & -i2\alpha_q \end{pmatrix}, \quad (\text{S37})$$

where the time dependence of the sources and partition labels are implied. We then expand Eq. (S36) to quadratic order in the fields as well as the sources around zero and find

$$\mathcal{S}^{(2)} = \frac{1}{2} \int_{t,t'} \langle v(t') | P(t) | v(t) \rangle, \quad (\text{S38})$$

where we define the vector $|v\rangle = (m_c, m_q, \alpha_c^A, \alpha_q^A, \alpha_c^B, \alpha_q^B, \beta_c^A, \beta_q^A, \beta_c^B, \beta_q^B)^T$. The kernel takes an upper-triangular, block matrix structure (upon symmetrization):

$$P = \begin{pmatrix} P_m & 2P_\alpha & 2P_\alpha & -2P_\beta & -2P_\beta \\ 0 & \frac{1}{8J^2}P_m & 0 & -\frac{1}{J}P_\beta & 0 \\ 0 & 0 & \frac{1}{8J^2}P_m & 0 & -\frac{1}{J}P_\beta \\ 0 & 0 & 0 & \frac{1}{8J^2}P_m & 0 \\ 0 & 0 & 0 & 0 & \frac{1}{8J^2}P_m \end{pmatrix}. \quad (\text{S39})$$

The block matrices have the same structure as the kernel in Eq. (S19). In fact, P_m is exactly equal to that kernel, and the components of the off-diagonal matrices are given by

$$P_\alpha^R(t) = P_\alpha^A(-t) = \frac{1}{4J} (P^R(t) + 2J\delta(t)), \quad (\text{S40})$$

$$P_\alpha^K(t) = \frac{1}{4J} P^K(t), \quad (\text{S41})$$

$$P_\beta^R(t) = P_\beta^A(-t) = 2J\Theta(t)e^{-\frac{\Gamma}{2}|t|} \cos(2\Delta t), \quad (\text{S42})$$

$$P_\beta^K(t) = -i2Je^{-\frac{\Gamma}{2}|t|} \sin(2\Delta t). \quad (\text{S43})$$

Equation (S38) being quadratic, we can integrate out the fields (after Fourier transformation) to obtain an action only in terms of the sources. This leads to the generating functional

$$W[\alpha_{c/q}^{A/B}, \beta_{c/q}^{A/B}] = -\frac{1}{2} \int_\omega \langle \tilde{v}(-\omega) | D(\omega) | \tilde{v}(\omega) \rangle, \quad (\text{S44})$$

where $|\tilde{v}\rangle = (\alpha_c^A, \alpha_q^A, \alpha_c^B, \alpha_q^B, \beta_c^A, \beta_q^A, \beta_c^B, \beta_q^B)^T$ and the kernel D is given by

$$D = \begin{pmatrix} D_{\alpha^A, \alpha^A} & 2D_{\alpha^A, \alpha^B} & 2D_{\beta^A, \alpha^A} & 2D_{\beta^A, \alpha^B} \\ 0 & D_{\alpha^A, \alpha^A} & 2D_{\beta^A, \alpha^B} & 2D_{\beta^A, \alpha^A} \\ 0 & 0 & D_{\beta^A, \beta^A} & 2D_{\beta^A, \beta^B} \\ 0 & 0 & 0 & D_{\beta^A, \beta^A} \end{pmatrix}. \quad (\text{S45})$$

There are only six independent kernels:

$$D_{\beta^A, \beta^A}(\omega) = -\frac{1}{8J^2} P_m(\omega) - P_\beta(\omega) P_m^{-1}(\omega) P_\beta(\omega), \quad (\text{S46})$$

$$D_{\alpha^A, \alpha^A}(\omega) = -\frac{1}{8J^2} P_m(\omega) + P_\alpha(\omega) P_m^{-1}(\omega) P_\alpha(\omega), \quad (\text{S47})$$

$$D_{\beta^A, \alpha^A}(\omega) = -\frac{1}{2J} P_\beta(\omega) + P_\beta(\omega) P_m^{-1}(\omega) P_\alpha(\omega), \quad (\text{S48})$$

$$D_{\beta^A, \alpha^B}(\omega) = P_\beta(\omega) P_m^{-1}(\omega) P_\alpha(\omega), \quad (\text{S49})$$

$$D_{\beta^A, \beta^B}(\omega) = -P_\beta(\omega)P_m^{-1}(\omega)P_\beta(\omega), \quad (\text{S50})$$

$$D_{\alpha^A, \alpha^B}(\omega) = P_\alpha(\omega)P_m^{-1}(\omega)P_\alpha(\omega). \quad (\text{S51})$$

All of the kernels are invariant under swapping the subscripts. The covariance matrix only requires static correlation functions, meaning we only want the D_{j_m, j_n}^K components (or derivatives of W with respect to $\alpha_q^{A/B}$ and $\beta_q^{A/B}$) for $j_m \in \{\alpha^A, \alpha^A, \beta^A, \beta^B\}$. In other words, the covariance matrix is actually given by (after performing the inverse Fourier transform)

$$C_{m,n} = -i \frac{\delta^2 W \left[\alpha_{c/q}^{A/B}, \beta_{c/q}^{A/B} \right]}{\delta j_{m,q}(t) \delta j_{n,q}(t)} \Big|_{\tilde{v}=0} = i D_{j_m, j_n}^K(0) = \langle X_m X_n \rangle. \quad (\text{S52})$$

The independent static correlation functions are (setting $J = 1$ for simplicity)

$$\langle q_c^A q_c^A \rangle = 1 + \frac{4\Delta}{\Gamma^2 - \Gamma_c^2}, \quad (\text{S53})$$

$$\langle q_c^A q_c^B \rangle = \frac{8\Delta}{\Gamma^2 - \Gamma_c^2}, \quad (\text{S54})$$

$$\langle p_c^A p_c^A \rangle = 1 - \frac{8(\Delta - 2)}{\Gamma^2 - \Gamma_c^2}, \quad (\text{S55})$$

$$\langle p_c^A p_c^B \rangle = -\frac{8(\Delta - 2)}{\Gamma^2 - \Gamma_c^2}, \quad (\text{S56})$$

$$\langle q_c^A p_c^A \rangle = \langle q_c^A p_c^B \rangle = \frac{2\Gamma}{\Gamma^2 - \Gamma_c^2}. \quad (\text{S57})$$

With the knowledge of the covariance matrix, we can then calculate the von Neumann entropy and entanglement measures such as entanglement negativity.

B. von Neumann Entropy

The von Neumann entropy for a given subsystem does not require the full 4×4 covariance matrix, only the 2×2 block corresponding to the chosen subsystem. We choose the subsystem A whose covariance matrix is given by

$$C^A = \begin{pmatrix} \langle q_c^A q_c^A \rangle & \langle q_c^A p_c^A \rangle \\ \langle p_c^A q_c^A \rangle & \langle p_c^A p_c^A \rangle \end{pmatrix} = \begin{pmatrix} 1 + \frac{4\Delta}{\Gamma^2 - \Gamma_c^2} & \frac{2\Gamma}{\Gamma^2 - \Gamma_c^2} \\ \frac{2\Gamma}{\Gamma^2 - \Gamma_c^2} & 1 - \frac{8(\Delta - 2)}{\Gamma^2 - \Gamma_c^2} \end{pmatrix}. \quad (\text{S58})$$

The symplectic eigenvalues of this matrix, $\pm\nu$, are given by the eigenvalues of $i\mathcal{J}C$ where [8]

$$\mathcal{J} = \begin{pmatrix} 0 & 1 \\ -1 & 0 \end{pmatrix}. \quad (\text{S59})$$

The von Neumann entropy can be then computed as [9]

$$S_{\text{vN}} = \frac{\nu + 1}{2} \log \left(\frac{\nu + 1}{2} \right) - \frac{\nu - 1}{2} \log \left(\frac{\nu - 1}{2} \right). \quad (\text{S60})$$

The positive symplectic eigenvalue of the matrix in Eq. (S58) is given by

$$\nu = \sqrt{\frac{12 + \Gamma^2 - \Gamma_c^2}{\Gamma^2 - \Gamma_c^2}}, \quad (\text{S61})$$

from which we find that, near a generic critical point ($\gamma \equiv \Gamma - \Gamma_c \ll \Gamma, J, \Delta$), the von Neumann entropy scales as $S_{vN} \sim \log(1/\sqrt{\gamma})$. At the weakly dissipative point ($\Gamma \ll J, \Delta$), we instead find $S_{vN} \sim \log(1/\Gamma)$. Invoking the finite-size scaling relations from the main text, we retrieve the $S_{vN} \sim \frac{1}{4} \log N$ behavior. Furthermore, somewhat identical analysis shows that the von Neumann entropy for the entire system (and not just the subsystems) has the same scaling behavior as $S_{vN} \sim \frac{1}{4} \log N$.

C. Logarithmic Negativity

To compute logarithmic negativity [10], one should take a partial transpose of the density matrix. For a Gaussian state, the partial transpose with respect to subsystem A , for example, is equivalent to sending $p^A \rightarrow -p^A$ in the covariance matrix [11]. The full matrix will not be reported as it is easily constructed from Eqs. (S53)-(S57) using the definition Eq. (S52). The logarithmic negativity, in terms of the symplectic eigenvalues ($\pm\nu_1, \pm\nu_2$), is [9]

$$E_{\mathcal{N}} = - \sum_i \log(\min(\nu_i, 1)). \quad (\text{S62})$$

We see that there is only one positive eigenvalue less than 1,

$$\nu = \left(1 + \frac{4}{\sqrt{\Gamma^2 + 16(\Delta - 1)^2}} \right)^{-1/2}, \quad (\text{S63})$$

which is equal to a constant $\nu = 1/\sqrt{2}$ along the entire phase boundary. This directly leads to $E_{\mathcal{N}} = \log \sqrt{2}$, as reported in the main text.

VI. NUMERICAL SIMULATION

A. Permutation Symmetric Basis

Performing exact numerics in driven-dissipative systems is a difficult task due to the exponential scaling of the Hilbert space with the system size. The Liouvillian matrix \mathbb{L} grows as $4^N \times 4^N$, making numerical simulations particularly hard. Alternatively, we take advantage of the permutation symmetry under which any two spins in Eq. (S2) can be exchanged without changing the dynamics. The steady state belongs to the fully-symmetric irreducible representation of the permutation group, so we introduce a permutation-symmetric basis [12, 13]

$$\rho_{N_x, N_y, N_z} = \frac{1}{\sqrt{N! N_x! N_y! N_z! N_I!}} \sum_{\mathcal{P}} \mathcal{P} (\sigma_1^x \otimes \dots \otimes \sigma_{N_x}^x \otimes \sigma_{N_x+1}^y \otimes \dots \otimes \sigma_{N_x+N_y}^y \otimes \sigma_{N_x+N_y+1}^z \otimes \dots \otimes \sigma_{N_x+N_y+N_z}^z \otimes I_{N_x+N_y+N_z+1} \otimes \dots \otimes I_N). \quad (\text{S64})$$

The sum $\sum_{\mathcal{P}}$ is over all permutations \mathcal{P} of the sites (the operator \mathcal{P} denotes the action of the permutation operator in the Hilbert space). These states are normalized as $\text{Tr}(\rho_{\mu} \rho_{\nu}) / 2^N = \delta_{\mu, \nu}$ where $\mu = (N_x, N_y, N_z)$. The Liouvillian matrix elements are given by

$$\mathbb{L}_{\mu, \nu} = \frac{1}{2^N} \text{Tr}(\rho_{\mu} \mathcal{L}[\rho_{\nu}]). \quad (\text{S65})$$

The action of the Liouvillian on a state can be determined analytically by inspecting how the total-spin operators act on one of our basis states:

$$\begin{aligned} S_x \rho_{N_x, N_y, N_z} &= \sqrt{N_x(N_I + 1)} \rho_{N_x-1, N_y, N_z} + i\sqrt{N_y(N_z + 1)} \rho_{N_x, N_y-1, N_z+1} \\ &\quad - i\sqrt{(N_y + 1)N_z} \rho_{N_x, N_y+1, N_z-1} + \sqrt{(N_x + 1)N_I} \rho_{N_x+1, N_y, N_z}, \end{aligned} \quad (\text{S66})$$

$$\begin{aligned} S_y \rho_{N_x, N_y, N_z} &= \sqrt{N_y(N_I + 1)} \rho_{N_x, N_y-1, N_z} + i\sqrt{N_z(N_x + 1)} \rho_{N_x+1, N_y, N_z-1} \\ &\quad - i\sqrt{(N_z + 1)N_x} \rho_{N_x-1, N_y, N_z+1} + \sqrt{(N_y + 1)N_I} \rho_{N_x, N_y+1, N_z}, \end{aligned} \quad (\text{S67})$$

$$\begin{aligned} S_z \rho_{N_x, N_y, N_z} &= \sqrt{N_z(N_I + 1)} \rho_{N_x, N_y, N_z-1} + i\sqrt{N_x(N_y + 1)} \rho_{N_x-1, N_y+1, N_z} \\ &\quad - i\sqrt{(N_x + 1)N_y} \rho_{N_x+1, N_y-1, N_z} + \sqrt{(N_z + 1)N_I} \rho_{N_x, N_y, N_z+1}, \end{aligned} \quad (\text{S68})$$

where $N_I = N - N_x - N_y - N_z$, and the action from the right can be found by taking the adjoint of the RHS. The only other non-trivial term is the dissipative term $\sum_i \sigma_i^- \rho \sigma_i^+$, whose action on the state is given by

$$\begin{aligned} \sum_i \sigma_i^- \rho_{N_x, N_y, N_z} \sigma_i^+ &= \frac{1}{2} [(N_I - N_z) \rho_{N_x, N_y, N_z} + \sqrt{N_z(N_I + 1)} \rho_{N_x, N_y, N_z-1} \\ &\quad - \sqrt{N_I(N_z + 1)} \rho_{N_x, N_y, N_z+1}]. \end{aligned} \quad (\text{S69})$$

Using the above relations, we find the action of the Liouvillian on the basis states to be

$$\begin{aligned} \mathcal{L}[\rho_{N_x, N_y, N_z}] &= \frac{4J}{N} \left(\sqrt{(N_x + 1)(N_y + 1)N_z} \rho_{N_x+1, N_y+1, N_z-1} \right. \\ &\quad + \sqrt{N_x(N_y + 1)N_z(N_I + 1)} \rho_{N_x-1, N_y+1, N_z-1} \\ &\quad - \sqrt{N_x N_y (N_z + 1)(N_I + 1)} \rho_{N_x-1, N_y-1, N_z+1} \\ &\quad \left. - \sqrt{(N_x + 1)N_y(N_z + 1)N_I} \rho_{N_x+1, N_y-1, N_z+1} \right) \\ &\quad + 2\Delta \left(\sqrt{N_x(N_y + 1)} \rho_{N_x-1, N_y+1, N_z} - \sqrt{N_y(N_x + 1)} \rho_{N_x+1, N_y-1, N_z} \right) \\ &\quad + \frac{\Gamma}{2} \left((N_I - N_z - N) \rho_{N_x, N_y, N_z} - 2\sqrt{(N_z + 1)N_I} \rho_{N_x, N_y, N_z+1} \right). \end{aligned} \quad (\text{S70})$$

Equipped with this expression, the matrix representing the Liouvillian can be quickly constructed using standard numerical techniques. In this basis, the dimensionality grows polynomially with the system size as $N(N+1)(N+2)/6 \sim \mathcal{O}(N^3)$ in contrast with the exponential growth in a generic many-body system. This scaling can also be contrasted with the $\mathcal{O}(N^4)$ growth of the usual Dicke (angular-momentum) basis. The steady state can be then obtained through the shifted-inverse-power method [14]. However, for larger system sizes ($N \gtrsim 90$) finding the steady-state by direct LU decomposition becomes inefficient. At that point, it is more efficient to use linear solvers like BICGSTAB to approximate the steady state.

To characterize dynamics, we investigate the correlation function $C(t) = \langle \{S_x(t), S_x(0)\} \rangle / N$ and response function $\chi(t) = i \langle [S_x(t), S_x(0)] \rangle / N$. The two-time expectation values can be calculated as [15]

$$\langle S_x(t) S_x(0) \rangle + \langle S_x(0) S_x(t) \rangle = \text{Tr} (S_x e^{t\mathcal{L}} [S_x \rho_{ss}]) + \text{Tr} (S_x e^{t\mathcal{L}} [\rho_{ss} S_x]) = 2\text{Re} \text{Tr} (S_x e^{t\mathcal{L}} [S_x \rho_{ss}]), \quad (\text{S71})$$

$$i(\langle S_x(t) S_x(0) \rangle - \langle S_x(0) S_x(t) \rangle) = i \text{Tr} (S_x e^{t\mathcal{L}} [S_x \rho_{ss}]) - i \text{Tr} (S_x e^{t\mathcal{L}} [\rho_{ss} S_x]) = -2\text{Im} \text{Tr} (S_x e^{t\mathcal{L}} [S_x \rho_{ss}]), \quad (\text{S72})$$

with ρ_{ss} being the steady-state density matrix. We can instead represent this in a vectorized form using our permutation symmetric basis,

$$C(t) = \frac{2}{N} \text{Re} \text{Tr} (S_x e^{t\mathcal{L}} [S_x \rho_{ss}]) = \frac{2}{N} \text{Re} \frac{\langle \langle S_x | e^{t\mathcal{L}} | S_x \rho_{ss} \rangle \rangle}{\langle \langle I | \rho_{ss} \rangle \rangle}, \quad (\text{S73})$$

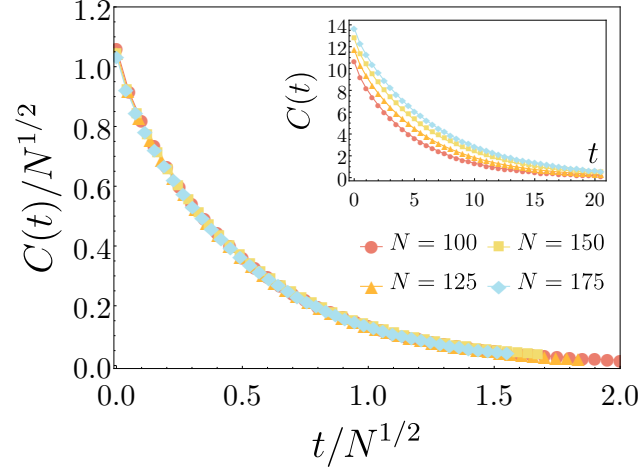


Figure S1: Finite-size scaling behavior of the driven-dissipative Ising model at a generic critical point ($J = 1, \Delta = 1, \Gamma = 4$). The critical dynamics is overdamped and is governed by a characteristic time scale that scales as $t \sim N^{1/2}$. This is in contrast with a weakly-dissipative critical point where the dynamics is underdamped with the scaling $t \sim N^{1/4}$ (see Fig. 3 in the main text).

$$\chi(t) = \frac{-2}{N} \text{Im Tr} (S_x e^{t\mathcal{L}} [S_x \rho_{ss}]) = \frac{-2}{N} \text{Im} \frac{\langle \langle S_x | e^{t\mathcal{L}} | S_x \rho_{ss} \rangle \rangle}{\langle \langle I | \rho_{ss} \rangle \rangle}, \quad (\text{S74})$$

where we have defined the vectorized state

$$|\rho(t)\rangle\rangle = \sum_{\mu} c_{\mu}(t) |\rho_{\mu}\rangle\rangle. \quad (\text{S75})$$

The denominator in Eq. (S73) is due to the normalization of the steady state (this is equivalent to dividing the state by $c_{0,0,0}$). In the case of static correlations, one can analytically show that the auto-correlation function takes the simple form

$$C(0) = \frac{2}{N c_{0,0,0}} \left(\sqrt{2N(N-1)} c_{2,0,0} + N c_{0,0,0} \right). \quad (\text{S76})$$

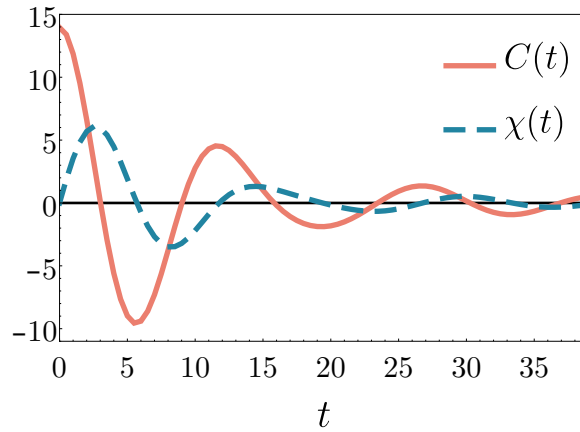


Figure S2: Correlation and response functions at the weakly dissipative critical point ($J = 1, \Delta = 2, \Gamma = 0.1$) from exact numerical simulation for $N = 100$. The classical fluctuation-dissipation relation [$\chi(t) = -\partial_t C(t)/2T_{\text{eff}}$] is satisfied for $T_{\text{eff}} = J = 1$. Specifically, every peak of the correlation function $C(t)$ coincides with a node of the response function $\chi(t)$.

Using these techniques, we were able to obtain the dynamical correlations at the weakly-dissipative critical point discussed in the main text. Here, we report the dynamical correlations at a generic critical point in Fig. S1. For completeness, we also compare the correlation and response functions at the weakly dissipative point in Fig. S2, where the effective fluctuation-dissipation relation becomes manifest.

B. Equilibrium Quantum Ising Model

In this section, we report the dynamics of the equilibrium infinite-range Ising model at finite temperature (in the absence of dissipation). Specifically, we demonstrate via exact numerical simulation that the thermal critical point of this model belongs to the same (static and dynamic) universality class as the driven-dissipative Ising model in the weakly dissipative regime. We start with the same Hamiltonian

$$H = -\frac{J}{N}S_x^2 + \Delta S_z. \quad (\text{S77})$$

This Hamiltonian features a thermal phase transition to an ordered phase where the Ising Z_2 symmetry is broken at the critical temperature [16]

$$T_c = \frac{2\Delta}{\ln\left(\frac{1+\Delta/2J}{1-\Delta/2J}\right)}. \quad (\text{S78})$$

The Hamiltonian conserves the total spin (i.e., $[H, \vec{S}] = 0$) which thus defines a good quantum number. In the angular-momentum basis defined by $|S, m\rangle$, the Hamiltonian becomes block diagonal with each block corresponding to a total spin S . However, each sector is highly degenerate with a multiplicity of $D(S)$. The multiplicity is given by $D(N/2) = 1, D(N/2 - 1) = N - 1, D(N/2 - 2) = N(N - 3)/2$, and

$$D(N/2 - p) = \frac{N(N - 1)\dots(N - p + 2)}{p!}(N - 2p + 1), \quad (\text{S79})$$

for $3 \leq p \leq N/2$ [16]. The thermal state is then given by

$$\rho(\beta) = e^{-\beta H} = \bigoplus_{S=0}^{N/2} \left(\bigoplus_{i=1}^{D(S)} e^{-\beta H_S} \right), \quad (\text{S80})$$

which is to be understood as the direct sum over each unique spin sector with the corresponding multiplicity $D(S)$. We then numerically calculate the correlation function

$$C(t) = \frac{1}{N} \langle \{S_x(t), S_x(0)\} \rangle = \frac{2}{N} \text{Re} \langle S_x(t) S_x(0) \rangle = \frac{2}{N} \text{Re} \text{Tr} (e^{-iHt} S_x e^{iHt} S_x \rho(\beta)). \quad (\text{S81})$$

A plot of the correlation function and its finite-size scaling behavior can be found in Fig. S3. There, we see that the dynamical exponent, defined via $t \sim N^\zeta$, is given by $\zeta = 1/4$ and that the dynamics is underdamped just like at the weakly-dissipative critical point of the driven-dissipative Ising model discussed in the main text.

C. Classical (stochastic) Ising model

For completeness, here we introduce the classical stochastic Ising model [17]. The (classical) Ising Hamiltonian is given by

$$\mathcal{H} = -\frac{J}{N}S^2, \quad (\text{S82})$$

where $S = \sum_i^N s_i$ with the Ising spin variable $s_i = \pm 1$. While the Hamiltonian (being a c number and commuting with all observables) does not impose any intrinsic dynamics, a stochastic, Glauber-type dynamics

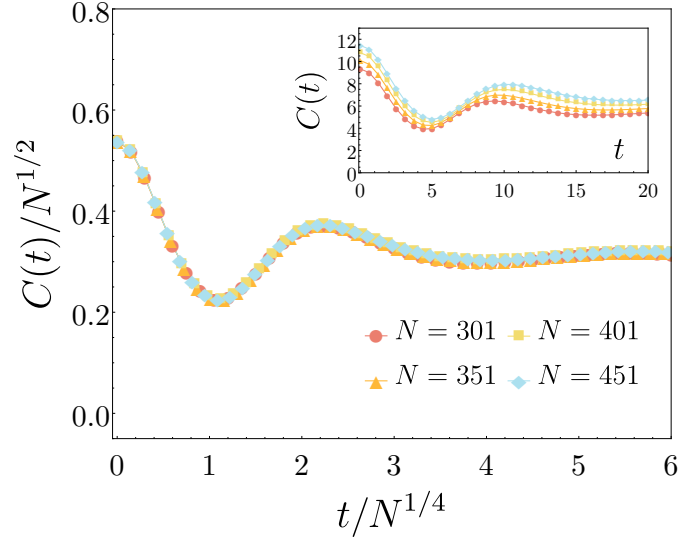


Figure S3: Finite-size scaling behavior of the infinite-range Ising model at a thermal critical point ($J = 1, \Delta = 1, T = 1.82048$). At this critical point, fluctuations scale as $N^{1/2}$, while the critical dynamics is underdamped and is governed by a characteristic time scale $t \sim N^{1/4}$. These exponents are identical to those of the driven-dissipative Ising model in the weakly dissipative regime (see Fig. 3 of the main text).

can be imposed via the (classical) master equation

$$\frac{d}{dt}P(\{s\}; t) = - \sum_{i=1}^N W(s_i \rightarrow -s_i, t)P(s_1, \dots, s_i, \dots, s_N; t) + \sum_{i=1}^N W(-s_i \rightarrow s_i, t)P(s_1, \dots, -s_i, \dots, s_N; t). \quad (\text{S83})$$

Here, $P(\{s\}; t)$ denotes the probability that the system is in a spin configuration $\{s\}$ at time t , and $W(s_i \rightarrow -s_i, t)$ represents the transition probability rate of a spin flip at site i and at time t . Under equilibrium conditions, the probability and transition rates satisfy the detailed balance [18],

$$W(s_i \rightarrow -s_i)P(s_1, \dots, s_i, \dots, s_N) = W(-s_i \rightarrow s_i)P(s_1, \dots, -s_i, \dots, s_N), \quad (\text{S84})$$

with the transition of the Glauber type (characterizing a non-conserved order parameter),

$$W(s_i \rightarrow -s_i) = \frac{1}{2\tau_0} [1 - s_i \tanh(\beta E)]. \quad (\text{S85})$$

Here, τ_0 defines the characteristic time scale of Glauber dynamics, and $E = -(2J/N) \sum_i^N s_j$. From here, one can simulate the relaxation of the system from a near-equilibrium state using Monte Carlo methods combined with the transition rate given above. Monte-Carlo simulations of the this model at criticality are consistent with a critical dynamical scaling where $t \sim N^{1/2}$ [17].

VII. CAVITY ADIABATIC ELIMINATION IN THE OPEN DICKE MODEL

In this section, we show that our model in Eq. (S2) follows from the open Dicke model in the limit of the large cavity detuning. This model is governed by the Hamiltonian [1]

$$H = \omega_0 a^\dagger a + \omega_z S_z + \frac{g}{\sqrt{N}} S_x (a + a^\dagger), \quad (\text{S86})$$

together with the dissipation given by the Lindblad operator $L_{\text{cav}} = \sqrt{\kappa} a$ representing the cavity loss as well as $L_i = \sqrt{\Gamma} \sigma_i$ characterizing atomic spontaneous emission. Here, ω_0 is the cavity detuning, ω_z is the atom

level splitting, and g is the atom-cavity coupling; again, $S_\mu = \sum_i \sigma_i^\mu$ is the total spin operator. The full quantum master equation then takes the form

$$\frac{d\rho}{dt} = -i[H, \rho] + \kappa \left(a\rho a^\dagger - \frac{1}{2}\{a^\dagger a, \rho\} \right) + \Gamma \sum_i \left(\sigma_i^- \rho \sigma_i^+ - \frac{1}{2}\{\sigma_i^+ \sigma_i^-, \rho\} \right). \quad (\text{S87})$$

Following the same steps as outlined in Sec. I (combined with a coherent-state representation for the cavity field), we obtain an action that consists of cavity, atomic and interaction terms:

$$\mathcal{S}_D = \mathcal{S}_{\text{cav}} + \mathcal{S}_{\text{int}} + \mathcal{S}_{\text{spin}}. \quad (\text{S88})$$

The cavity term in the action is given by

$$\mathcal{S}_{\text{cav}} = \int_\omega (a_c^*(\omega) \ a_q^*(\omega)) \begin{pmatrix} 0 & \omega - \omega_0 - i\frac{\kappa}{2} \\ \omega - \omega_0 + i\frac{\kappa}{2} & i\kappa \end{pmatrix} \begin{pmatrix} a_c(\omega) \\ a_q(\omega) \end{pmatrix}. \quad (\text{S89})$$

Defining $a = (x - ip)/2$, we can integrate out the imaginary component of the cavity field, p , exactly as S_{int} does not depend on p . Tracing out the spins (see Sec. I), we then find an *exact* expression for the action

$$\mathcal{S}_D = \int_\omega \langle x(-\omega) | D(\omega) | x(\omega) \rangle - iN \ln \text{Tr} \left(\mathcal{T} e^{\int_t \mathbb{T}_D(x_c/q(t))} \right), \quad (\text{S90})$$

where $|x(\omega)\rangle = (x_c(\omega), x_q(\omega))^T$ and the kernel $D(\omega)$ is given by

$$D(\omega) \equiv \begin{pmatrix} 0 & D^A(\omega) \\ D^R(\omega) & D^K(\omega) \end{pmatrix} = \begin{pmatrix} 0 & \frac{1}{4} \left(-\frac{(\kappa+2i\omega)^2}{4\omega_0} - \omega_0 \right) \\ \frac{1}{4} \left(-\frac{(\kappa-2i\omega)^2}{4\omega_0} - \omega_0 \right) & \frac{i\kappa(\kappa^2+4(\omega^2+\omega_0^2))}{16\omega_0^2} \end{pmatrix}. \quad (\text{S91})$$

The matrix \mathbb{T}_D is rather similar to that in Eq. (S13):

$$\mathbb{T}_D(x_c(t), x_q(t)) = \begin{pmatrix} -\frac{\Gamma}{4} - i\frac{2\sqrt{2}g}{\sqrt{N}}x_q(t) & i\omega_z & -i\omega_z & \frac{\Gamma}{4} \\ i\omega_z - \frac{\Gamma}{2} & -\frac{3\Gamma}{4} - i\frac{2\sqrt{2}g}{\sqrt{N}}x_c(t) & -\frac{\Gamma}{4} & -i\omega_z - \frac{\Gamma}{2} \\ -i\omega_z - \frac{\Gamma}{2} & -\frac{\Gamma}{4} & -\frac{3\Gamma}{4} + i\frac{2\sqrt{2}g}{\sqrt{N}}x_c(t) & i\omega_z - \frac{\Gamma}{2} \\ \frac{\Gamma}{4} & -i\omega_z & i\omega_z & -\frac{\Gamma}{4} + i\frac{2\sqrt{2}g}{\sqrt{N}}x_q(t) \end{pmatrix}. \quad (\text{S92})$$

We then make the transformation $m_c \equiv (D_0^R x_c + D_0^K x_q)/\sqrt{N}g$ and $m_q \equiv D_0^R x_q/\sqrt{N}g$ with $D_0 \equiv D(\omega=0)$, and further define $J \equiv g^2/D_0^R = 16g^2\omega_0/(\kappa^2 + 4\omega_0^2)$, $\Gamma_x \equiv J\kappa/\omega_0$, and $\Delta \equiv \omega_z$. The action is then cast as

$$\tilde{\mathcal{S}} = \int_\omega \langle m(-\omega) | P(\omega) | m(\omega) \rangle - iN \ln \text{Tr} \left(\mathcal{T} e^{\int_t \tilde{\mathbb{T}}(m_c/q(t))} \right), \quad (\text{S93})$$

where $|m(\omega)\rangle = (m_c(\omega), m_q(\omega))^T$, the kernel P is given by

$$P(\omega) = -N \begin{pmatrix} 0 & J(1 + \frac{4i\kappa\omega - 16\omega^2}{\kappa^2 + \omega_0^2}) \\ J(1 - \frac{4i\kappa\omega + 16\omega^2}{\kappa^2 + \omega_0^2}) & i\Gamma_x(1 + \frac{4\omega^2}{\kappa^2 + 4\omega_0^2}) \end{pmatrix}, \quad (\text{S94})$$

and the matrix $\tilde{\mathbb{T}}$ is given by

$$\tilde{\mathbb{T}}(m_c(t), m_q(t)) = \mathbb{T}(m_c(t), m_q(t)) + \mathbb{T}_x(m_q(t)), \quad (\text{S95})$$

with \mathbb{T} identical to the matrix in Eq. (S13) and

$$\mathbb{T}_x(m_q(t)) = \begin{pmatrix} 0 & 0 & 0 & 0 \\ 0 & -2\sqrt{2}\Gamma_x m_q(t) & 0 & 0 \\ 0 & 0 & 2\sqrt{2}\Gamma_x m_q(t) & 0 \\ 0 & 0 & 0 & 0 \end{pmatrix}. \quad (\text{S96})$$

Now we consider the limit of large ω_0 and κ , in which case we can ignore those terms in Eq. (S94) that are suppressed by a factor of $1/(\kappa^2 + \omega_0^2)$. This eliminates the frequency-dependent terms and yields the kernel

$$P(\omega) \approx -N \begin{pmatrix} 0 & J \\ J & i\Gamma_x \end{pmatrix}. \quad (\text{S97})$$

Using the quantum-to-classical mapping, one can show that the diagonal term ($\sim i\Gamma_x$) can be identified with dephasing in the form of the Lindblad operator $L_x = \sqrt{\Gamma_x/N} S_x$. Indeed, this agrees with the large-detuning limit discussed in Ref. [19]. Our model is different, however, due to the atomic spontaneous emission, which allows for a nontrivial steady state. To obtain the driven-dissipative Ising model, we can consider the detuning ω_0 to be the largest frequency scale even compared to κ . In this scenario, we can neglect the dephasing term since $\Gamma_x = J\kappa/\omega_0 \ll J$. In the limit, we recover the driven-dissipative Ising model introduced in Eq. (S12).

-
- [1] E. G. Dalla Torre, S. Diehl, M. D. Lukin, S. Sachdev, and P. Strack, *Phys. Rev. A* **87**, 023831 (2013).
 - [2] A. Kamenev, *Field Theory of Non-Equilibrium Systems* (Cambridge University Press, 2011).
 - [3] L. M. Sieberer, M. Buchhold, and S. Diehl, *Rep. Prog. Phys.* **79**, 096001 (2016).
 - [4] U. C. Täuber, *Critical Dynamics: A Field Theory Approach to Equilibrium and Non-Equilibrium Scaling Behavior* (Cambridge University Press, 2014).
 - [5] V. Eisler and Z. Zimboras, *New J. Phys.* **16**, 123020 (2014).
 - [6] I. Peschel and V. Eisler, *J. Phys. A* **42**, 504003 (2009).
 - [7] I. Peschel, *J. Phys. A* **36**, L205 (2003).
 - [8] A. Serafini, F. Illuminati, and S. D. Siena, *J. Phys. B* **37**, L21 (2003).
 - [9] G. Adesso, A. Serafini, and F. Illuminati, *Phys. Rev. A* **70**, 022318 (2004).
 - [10] G. Vidal and R. F. Werner, *Phys. Rev. A* **65**, 032314 (2002).
 - [11] J. Eisert, M. Cramer, and M. B. Plenio, *Rev. Mod. Phys.* **82**, 277 (2010).
 - [12] Z.-X. Gong, M. Xu, M. Foss-Feig, J. K. Thompson, A. M. Rey, M. Holland, and A. V. Gorshkov, [arXiv:1611.00797](https://arxiv.org/abs/1611.00797) (2016).
 - [13] P. Kirton and J. Keeling, *Phys. Rev. Lett.* **118**, 123602 (2017).
 - [14] P. D. Nation, [arXiv:1504.06768](https://arxiv.org/abs/1504.06768) (2015).
 - [15] C. Gardiner and P. Zoller, *Quantum Noise: A Handbook of Markovian and Non-Markovian Quantum Stochastic Methods with Applications to Quantum Optics*, 3rd ed. (Springer, 2004).
 - [16] A. Das, K. Sengupta, D. Sen, and B. K. Chakrabarti, *Phys. Rev. B* **74**, 144423 (2006).
 - [17] S. K. Oh, *J. Korean Phys. Soc.* **48**, 18 (2006).
 - [18] J. Cardy, *Scaling and Renormalization in Statistical Physics* (Cambridge University Press, 1996).
 - [19] F. Damanet, A. J. Daley, and J. Keeling, *Phys. Rev. A* **99**, 033845 (2019).